Design and Demonstration of Micro-mirrors and Lenses for Low Loss and Low Cost Single-Mode Fiber Coupling in 3D Glass Photonic Interposers

Bruce C Chou, William Vis, Bilal Khan, Fuhan Liu, Venky Sundaram, and Rao Tummala
3D Systems Packaging Research Center
Georgia Institute of Technology
Atlanta, GA, USA
e-mail: cchou36@gatech.edu

Ryuta Furuya
Systems Solution Division
Ushio Inc.
Tokyo, Japan
e-mail: rfuruya3@mail.gatech.edu

Abstract—**This paper presents the first demonstration of a novel fiber coupling structure that enables low-loss and low-cost fiber coupling in an ultra-miniaturized 3D glass photonic interposer. The novel 3D coupling structure consists of a tapered optical waveguide with an integrated lensed turning mirror on one end and a cylindrical lens on the other end, in a 150 µm glass substrate. The lens waveguide and turning mirror provide coupling loss of <0.5 dB and 90% tolerance of 2 µm for out-of-plane coupling between a Photonic Integrated Circuit and a single-mode fiber. The lens waveguide is fabricated using planar lithography to reduce overall cost. In addition, precision U-grooves in glass are employed to allow for a coefficient of thermal expansion matched interface between the fiber and the substrate, thus enabling low-cost passive alignment.**

Keywords- optical waveguide, micro-lens, micro-mirror, moving mask lithography, optical fiber assembly

I. INTRODUCTION

As the bandwidth demand for IP traffic continues to rise, a substantial increase in network capacity at all levels of communication is expected [1]. While optics has been the backbone for telecommunication due to its higher capacity and lower loss over long distances, it has not penetrated shorter distance communication due to the overhead loss and the high cost of integration. The overhead loss comes from electro-optical conversion and the coupling of optical components, and it is largely independent of transmission distance. The high cost of integration comes from the inherent heterogeneous system consisting of both electrical and optical devices, which will remain so as long as light generation in silicon remains elusive [2].

Two major contributors to high cost and high loss, respectively, are the active alignment of single-mode fibers (SMF), and the fabrication of coupling structures required to improve the direct coupling loss between optical fibers and photonic dies. Without any coupler, the direct coupling loss from a SMF to Photonic Integrated Circuit (PIC) waveguide (WG) can be as high as ~20 dB due to the large mode mismatch between WG core (~0.2 μm^2) and SMF core (>50 μm^2). The two primary fiber coupling mechanisms are in-plane and out-of-plane, where in-plane edge coupling using inverse taper WGs is well-developed with reported coupling loss of 0.8 dB [3].

Out-of-plane coupling to surface emitting devices is the preferred integration method due to the combined attributes of ease of coupling and compact form-factor. The emergence of vertical grating couplers (VGC) also added to the importance of this type of coupling [4]. Out-of-plane vertical grating coupling directly to angled polished fiber have demonstrated about 2 dB loss; however, active fiber alignment with highly precise tilt was required as no registration marks were present on the PIC die [5]. While passive aligned structures have been proposed, the height and angle requirement offset the potential benefits [6]. In addition, out-of-plane coupling necessitates a turning mirror, for which no simple fabrication method exists. Angle polished fiber, ultra-precision machining (UPM), molding, or laser ablation can produce the required precision, but lack scalability [5], [7] – [9].

The novel out-of-plane turning structure and U-groove alignment structure proposed and demonstrated in this paper overcomes the high integration cost while achieving low coupling loss. The novel structure utilizes the 3D Glass Photonics (3DGP) interposer technology by taking advantage of the dimensional stability, optical transparency, and coefficient of thermal expansion (CTE) matching of glass comparing to properties of silicon or organic substrates [10]. This paper is the first reporting of the full coupling structures after the initial report on the fabrication of turning waveguides [11]. A diagram for system-level integration is shown in Figure 1. The novel coupling structure consists of three parts:

1. A lens waveguide consisting of two convex lenses capping an optical waveguide.
2. A planar processed integrated turning mirror using moving mask lithography [12].
3. U-groove structures made directly on glass.

Plano-convex lens can be fabricated directly on glass by a polymer reflow process. The reflow process can produce lens of consistent curvature within 2 degrees. Moving-mask lithography is a planar and parallel process that can be used to make slanted mirrors, with angular control of 1.5° achieved over the entire panel. Both 45° and 40° turning have been realized, thus accommodating vertical and 10° offset wave coupling, respectively, to flip-chip bonded PIC.

978-1-5090-1204-6/16 $31.00 © 2016 IEEE
DOI 10.1109/ECTC.2016.332

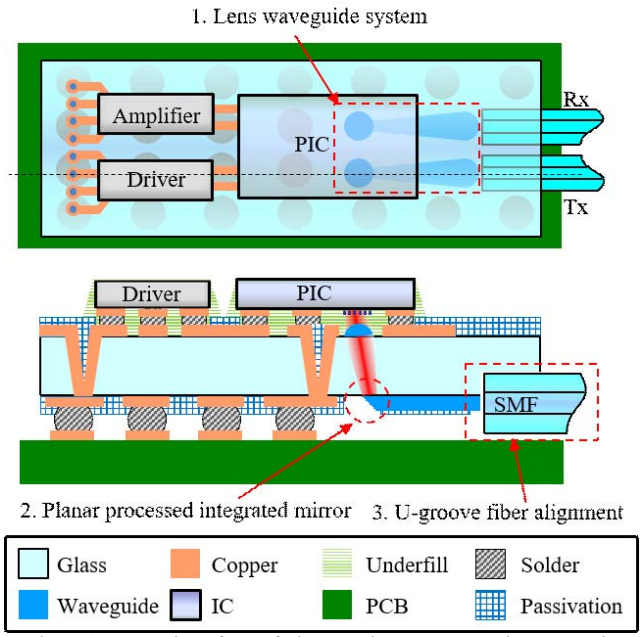

Figure 1. Integration of out-of-plane turning structure and U-groove in glass interposer, for coupling between a gratings based PIC and a SMF.

U-grooves formed on glass by mechanical dicing enables single-fiber alignment with precise x, y, θ_x, and θ_y control to the lens waveguide. The coupling structure is designed to work with vertical cleaved fiber requiring no angle polishing process step.

II. Initial Process Development

Initial process data was collected to help determining the design rules. CYCLOTENE™ 6505, a positive-toned optical polymer based on Benzocyclobutene (BCB) chemistry, developed by Dow Chemical, was chosen as the core material and lens material. The cladding layer chosen was a dry-film material, also by Dow Chemical, with properties similar to CYCLTENE™ 4000s [13]. The glass substrate was provided by Corning Inc. The selected properties of these materials are listed in Table I. Since the 6505 is a liquid polymer, the achievable thickness can vary from 4 to 7 µm depending on spin speed.

Since it is positive-toned, the highest angle achieved in the initial process development was 77°, as shown in Figure 2a. By performing an exposure ladder, a linear relationship was determined between the waveguide height, h_w, and exposure dose, D, up to 400 mJ/cm^2 as follows:

$$h_w = 0.0167D. \quad (1)$$

The linear relationship means this material is suitable for moving mask lithography, where an angled sidewall can be achieved by moving the mask along the length of the sidewall during exposure. The UX-44101 projection aligner from Ushio Inc. was programmed to move the mask during lithography. The resulting 45° turning structure is shown in Figure 2b.

TABLE I. Selected Properties of Materials Used

Material	CYCLOTENE 6505	Dry-film CYCLOTENE	Corning SGW3
R.I. @ 1550 nm	1.5575	1.543	1.4935
Tg	300 C	>300 C	670 C
CTE (ppm/C)	45	63	3.2
Thickness	4 – 7 µm	10 µm	150 µm

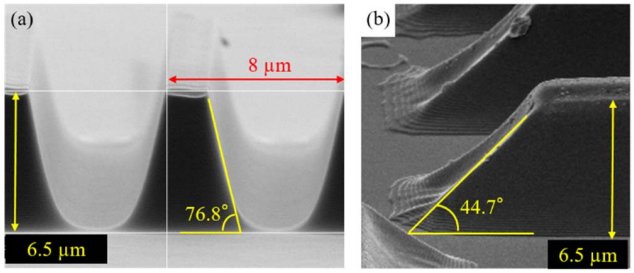

Figure 2. (a) Standard optical waveguide using CYCLOTENE 6505, and (b) planar processed turning mirror using moving mask method.

III. Modeling and Design

The coupling between two single-mode structures can be modeled by a Gaussian beam. As the beam expands along an unguided region, the longitudinal coupling loss, $\kappa(z)$, is described as a function of the distance, z, as follows:

$$\kappa(z) = \frac{4r_0^2 r_1^2}{(r_0^2 r_1^2)^2 + (\lambda z / \pi n_0)^2} \quad (2)$$

where r_0 and r_1 are the mode field radius of the source and the destination, λ is the wavelength of the light, and n_0 is the refractive index of the unguided region. The overall coupling efficiency is obtained by taking into account the lateral and angular displacements:

$$\eta = \kappa(z)\exp(-\kappa(z)\{\frac{x^2}{2}(\frac{1}{r_0^2}+\frac{1}{r_1^2}) + \frac{\pi^2\theta^2}{2\lambda^2}[r_g^2(z)+r_1^2] - \frac{x\theta z}{r_0^2}\}), \quad (3)$$

where $r_g(z)$ indicates the beam divergence away from the source given by

$$r_g^2(z) = r_0^2 + (\frac{\lambda z}{\pi n_0 r_0})^2. \quad (4)$$

A lens can be used to match the mode field and minimizing the effects of beam divergence by transforming r_0, to match r_1 at a certain distance depending on the focal length of the lens. Similarly, an adiabatically tapered waveguide can match the r_0 and r_1 at the two ends of the taper. The coupling efficiency and alignment tolerance with respect to x, θ, and z can therefore be optimized by a combination of waveguides and lenses.

The turning structure, shown in Figure 3a, was designed to achieve the turning by total-internal-reflection (TIR) of polymer-air interface to eliminate the metallization step.

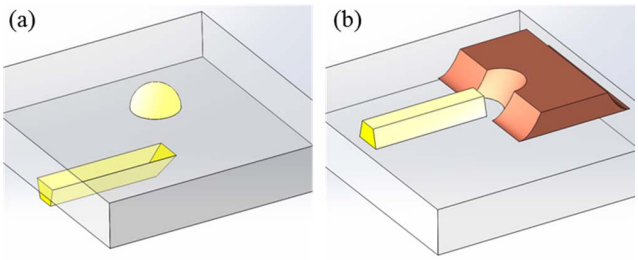

Figure 3. Design of (a) TIR and (b) metallic turning structures.

However, the turned light wave had to travel through a glass substrate at least 100 µm thick. Precision alignment of turning structure to the plano-convex lens on the top side of the glass is necessary to ensure good coupling. As a result, a second design, shown in Figure 3b, was proposed to achieve turning by conventional reflection of metal interface. In this design, moving mask method would be used to make the turning mirror only.

The coupling efficiency and tolerance of the two designs were modeled using a combination of OptiFDTD and OptiBPM software. FDTD (Finite Difference Time Division) method was used to model the turning structures, while BPM (Beam Propagation Method) was used for fiber alignment to tapered and lensed waveguide.

A. Waveguide Geometry

The single-mode condition of the turning waveguide structure was determined based on the refractive indices of the core, cladding, and substrate materials used, as listed in Table I. The mode solver in OptiBPM was used to determine the largest waveguide cross-section that ensures single-mode condition. For a height of 6.5 µm at 77° sidewall angle, the maximum top waveguide width was determined to be 6 µm. All subsequent designs would assume this waveguide dimension unless otherwise stated.

B. Turning Mirror

The sidewall achieved by moving mask method, for example in Figure 2b, were consistently concaved due to the natural reflowing of the polymer material. It was curve-fitted by an exponential tapering function with $\alpha = 0.5$. 2D FDTD modeling was performed using this sidewall geometry to determine the turning loss and the angular sensitivity, with the results shown in Figure 4 and Figure 5, respectively. The turning loss at exactly 45° were 0.62 dB and 0.17 dB, respectively. The 0.45 dB higher loss of TIR mirror was evident in the visible radiation loss at the waveguide-to-glass interface along the concaved sidewall. If the sidewall was straight, the simulated loss was less than 0.5 dB. On the other hand, the concaved shape of the metallized mirror actually helped focusing the light. The angular sensitivity of TIR mirror was as expected, with 1 dB tolerance at ±4°. The efficiency of the metallic mirror did not change significant from angle variation, which was attributed to the focusing function of the concave mirror. Despite the addition process steps, metallic mirror was clearly the superior design.

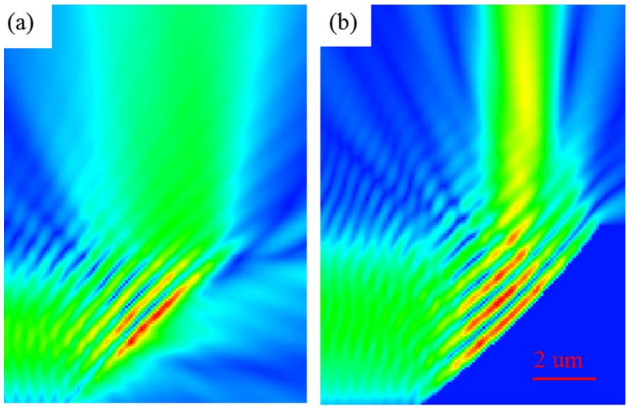

Figure 4. 2D FDTD simulation results for (a) TIR and (b) metallic turning structures with accurately modeled sidewall profile.

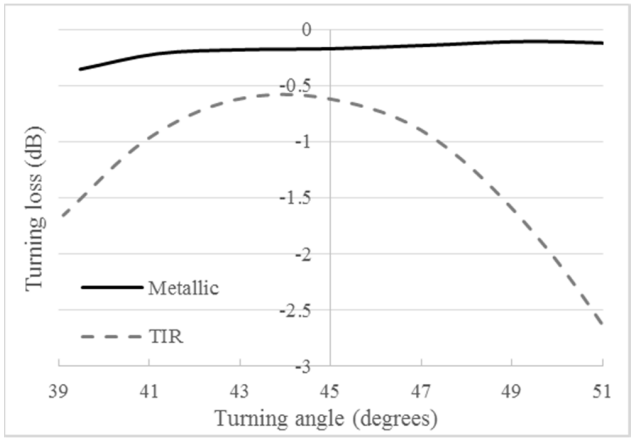

Figure 5. Turning loss sensitivity with respect to turning angle, for both metallic and TIR mirrors.

C. Fiber Coupling

The coupling loss and misalignment tolerance of waveguide-to-fiber interface was modeled by 3D BPM. The waveguide end was tapered to 10 µm width to match the mode field radius of SMF. At perfect alignment and 20 µm gap, the simulated coupling loss was 0.4 dB, which was due to the distance (0.15 dB) and the mismatched height (6.5 µm comparing to 8.2 µm in a standard SMF). The 1-dB tolerance was found to be 2.5 µm in the x direction and 2 µm in the y direction, as shown in Figure 6. The x-direction tolerance is on par with fiber-to-fiber coupling due to the tapered waveguide design, whereas the y-direction tolerance is limited by the achievable thickness of the optical waveguide, which cannot be tapered easily using planar processes. Similar modeling was done with respect to the tilt, where the 1-dB tolerance was found to be 2°. Lastly, the z-direction tolerance is 40 µm, and for the application θ_z alignment is not needed. A cylindrical lens at the end of the waveguide could improve the coupling loss to 0.3 dB, and improve the z-direction tolerance, but it would decrease the alignment tolerance for x and θ_x.

Table II summarizes the turning and fiber coupling structures discussed above.

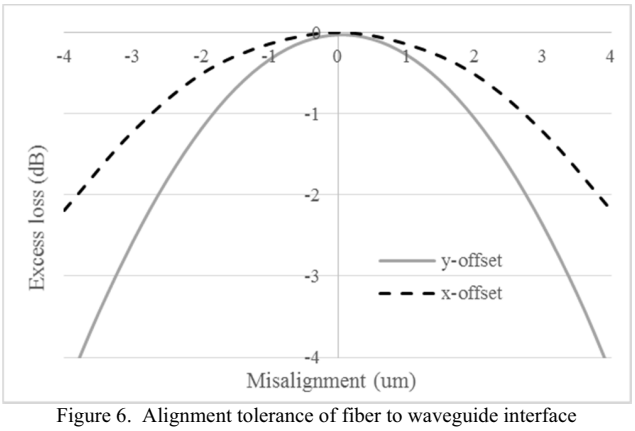

Figure 6. Alignment tolerance of fiber to waveguide interface

TABLE II. LOSSES AND TOLERANCES OF OPTICAL STRUCTURES

Turning mirror	**TIR**	**Metallic**
Min coupling loss	0.62 dB	0.17 dB
Angle sensitivity	±4° @ 1 dB	Insensitive
Process steps	Two steps: moving mask (MM), reflow lens	Three steps: MM, mirror coating, normal litho.
Process req.	Lens-to-mirror alignment through glass: <3 µm	Lens-to-WG: x direction alignment <2 µm
Waveguide end	**Straight taper**	**Lensed taper**
Min coupling loss	0.4 dB	0.25 dB
x & y 1 dB tol.	2.5 µm & 2 µm	2 µm & 2 µm
θ_x & θ_y 1 dB tol.	2° & 1.6°	1.6° & 1.6°
z 1 dB tolerance	40 µm	> 80 µm

A metallic mirror with a tapered lens waveguide would achieve the lowest coupling loss of 0.42 dB, with alignment requirement at 2 µm for both device fabrication and fiber placement. Currently, 2 uµm resolution in device fabrication at panel level can be achieved.

IV. FABRICATION AND CHARACTERIZATION

A. *Turning Waveguide Fabrication*

Two process sequences were developed for the TIR mirror and metallic mirror, respectively. For the TIR mirror, the turning waveguides were photo-lithographically formed on glass using moving mask method, then soft-cured. The cladding layers, which also acted as passivation layers for the electrical layers, were laminated on both sides, patterned photo-lithographically, and soft cured. Finally, micro-lenses were formed by reflow process on the top side of the glass, and hard cured. All of the optical structures were formed using planar lithographic process. Completed TIR structure integrated with electrical pads is shown in Fig. 7.

For the metallic mirror, the turning structures were photo-lithographically formed then hard cured. Ti-Cu coating were patterned on the sidewalls using sputtering and subtractive etching. The waveguides were formed using normal lithography, then soft cured. The cladding layers were applied similar to the TIR case. The completed structure, prior to cladding application is shown in Figure 8.

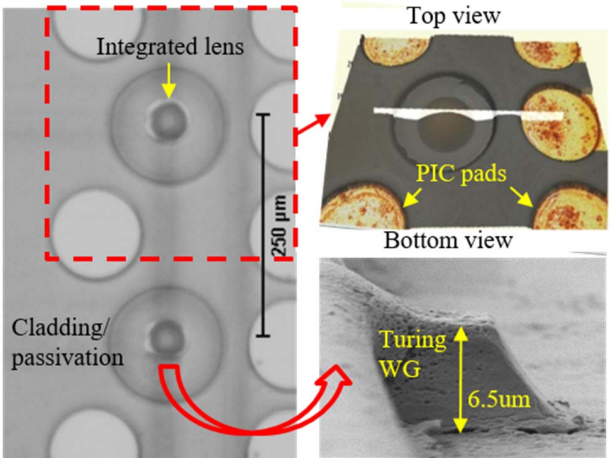

Figure 7. Fabricated TIR coupling structure viewed from top with SEM micrograph of the turning structure at the bottom and confocal micrograph of the lens on top with electrical connections to laser chip.

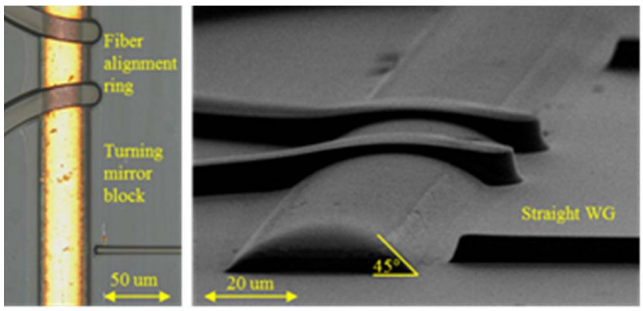

Figure 8. Fabricated metallic coupling structure viewed from top (left) and viewed in SEM.

The alignment of TIR mirrors to integrated lens was measured over the entire panel. The average misalignment was 3.8 µm, which exceeded the process requirement as listed in TABLE II. Currently, no simple solution exists to improve the alignment of structures between the top side and the bottom side of glass. On the other hand, the average misalignment between the waveguides and metallic turning mirror measured less than 1 µm, as alignment was fully planar.

B. *U-Groove Formation*

Two u-groove formation techniques were tried on glass, both by mechanical dicing, in collaboration with DISCO Corporation. The two techniques were as follows: Shallow groove cut and through slot cut with glass-glass bonding. The dicing saw in DISCO Corp. could achieve shallow grooves at 1 µm level precision in depth (y-direction), as shown in Figure 9, which would be within the alignment tolerance. However, the rounded nature of the dicing saw meant the two edges of the groove would be rounded corresponding to the diameter of the blade. For a 58 µm deep groove with a 6 cm blade, the tapered region would be 1.4 mm long. As such, the groove method could not establish fiber end, and could not be used directly.

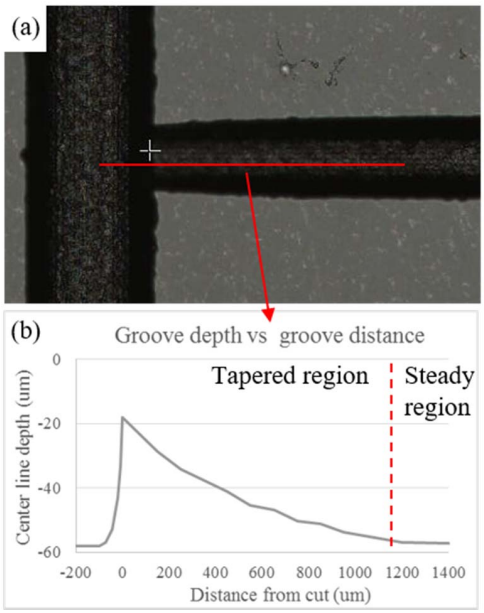

Figure 9. U-groove formation by shallow cut, with extended tapered region.

The well-controlled thickness of thin glass substrate was used to achieve y-direction alignment in the through slot cut technique. The measured sidewall angle from the cut is 88.2° with standard deviation of 0.3°.

The glass with cut slots were then bonded to an uncut glass by a polymer adhesive. In this study, EPR-129 photo-definable polymer adhesive being developed by MircoChem Corp. was chosen for its simple processing and low temperature curing. The process steps were as follows:

1) The glass surface was cleaned by solvents and plasma etching.

2) The EPR-129 material was spin coated on, and soft-baked to remove excess solvents.

3) The material was exposed at i-line.

4) (Optional) The material was developed in Tetramethylammonium hydroxide (TMAH) and baked dry.

5) The bonding was accomplished in a planarizer provided by Brewer Science Inc. to a desired pressure.

6) The bonded sample was then cured and diced to allow fiber coupling.

The initial trial was done on slots cut on a 100 µm glass bonded to a 50 µm glass as shown in Figure 10a. 100 µm glass was chosen for slot cut due to handling concerns with 50 µm glass. Process improvement is underway to enable 50 µm glass cutting. Due to the mismatched height, the slot needed to be cut less than 125 µm to allow for correct y-direction placement of fiber, as shown in in Figure 10b. The cut achieved averaged 120 µm with less than 2 µm standard deviation. The measured y-direction offset averaged 1.48 µm, with a standard deviation of 1.5 µm, while the x-direction offset from center was 5.5 µm with a standard deviation of 4.8 µm. The high variation in the x-direction was primarily due to the lack of a suitable fiber bonding equipment at the moment.

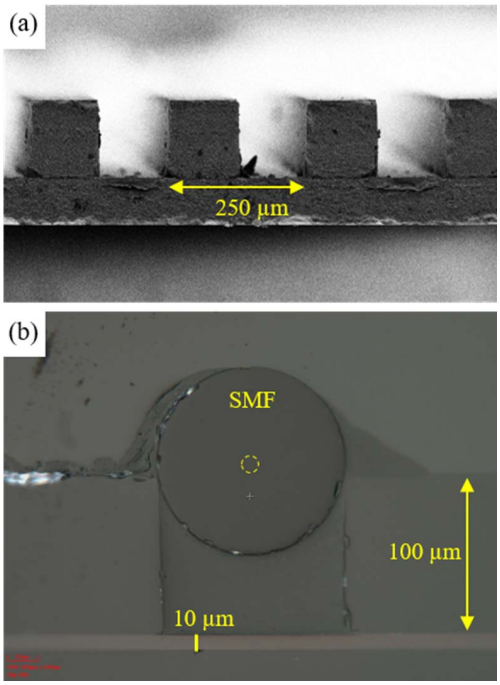

Figure 10. U-groove formation by through slot cut. (a) SEM micrograph of the grooves and (b) cross-section of fiber assembled on one of the grooves.

The fiber alignment trial was performed on an x-y-z micropositioner normally used for optical measurement. Fiber was placed, then epoxy was dispensed and filled by capillary action, but no UV cure was done since no UV source was available near the optical measurement setup.

The precision achieved with the initial trial was not yet enough to allow passive alignment of optical fibers, as the x-direction misalignment was greater than 5 µm. As discussed, the two main reasons were a lack of fiber assembly tools currently in GT-PRC's lab and the difficulties in cutting 50 µm glass, which can establish reliable y-direction height, thus simplifying the alignment scheme.

C. Integration with Electrical Interconnections

An integrated test vehicle incorporating optical, thermal, and electrical circuitry was designed to demonstrate a fully functional optical transceiver module as shown in Figure 1. The proposed process flow is shown in Figure 11. This process flow did not include u-groove structures, as they were still in development phase as discussed in the previous section.

The electrical fabrication process was already described in a previous publication by the authors [14]. In short, through glass vias (TGVs) were formed by Corning using their proprietary process on a 150 µm glass. Then, copper seed layer was sputtered on both sides, on top of a thin (50 nm) titanium adhesion layer. The electrical metallization was accomplished by a semi-additive process, where 5 µm of copper metallization was electrolytic plated. The optical layers were added after, with the process described in Section IV.A.

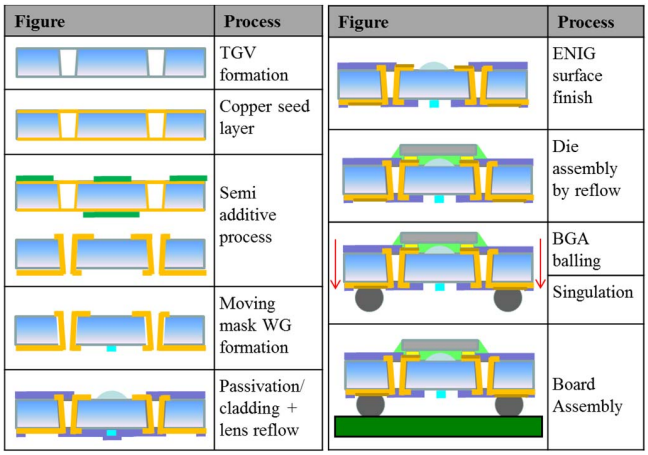

Figure 11. Process flow for the integrated test vehicle with out-of-plan turning structure.

It should be noted that reflow lenses were sensitive to curing profile, and a specific profile was developed by the authors to achieve the desired shape. After fully curing the optical layers, electroless nickel and immersion gold (ENIG) surface finish was applied to the exposed copper, to allow for die assembly, singulation, and board assembly.

Completed test vehicle is shown in Figure 12. The panel used was 150 µm thick and measured 100 mm by 100 mm. This dimension was suited for in-house processes, as the exposure tool only has an active diameter of 100 mm. The coupon, measured 16 mm by 16 mm, contained high speed electrical test structures, thermal dissipation structures, and the out-of-plane turning structures based on TIR mirrors. The center of the coupon was reserved for a thermal test chip capable of emulating power generated by a PIC transmitter, while the four corners were reserved for VCSEL assembly for active measurement of optoelectronic devices. Currently, die assembly is underway in preparation for singulation and reliability testing.

V. Conclusion

This paper presented the first design, panel level fabrication, and characterization of a novel out-of-plane fiber coupling structure in a 150 µm thick glass interposer. The polymer based tapered waveguide structure featuring metallic turning mirror or total-internal-reflection turning mirror could achieve < 0.5 dB or < 1 dB coupling loss from SMF to photonic IC, respectively. The tapered waveguide with a cylindrical lens could increase z-directional alignment tolerance at a relatively small penalty in x- and y- alignment, which were at fiber-to-fiber level thanked to the tapered waveguide design. The waveguide structures were integrated in a test vehicle with electrical components using mostly panel level process, thus proving feasibility of low cost fabrication. U-groove structures in glass were explored fiber to allow low-cost passive fiber alignment; however, at the moment the results had not yet achieve the precision required.

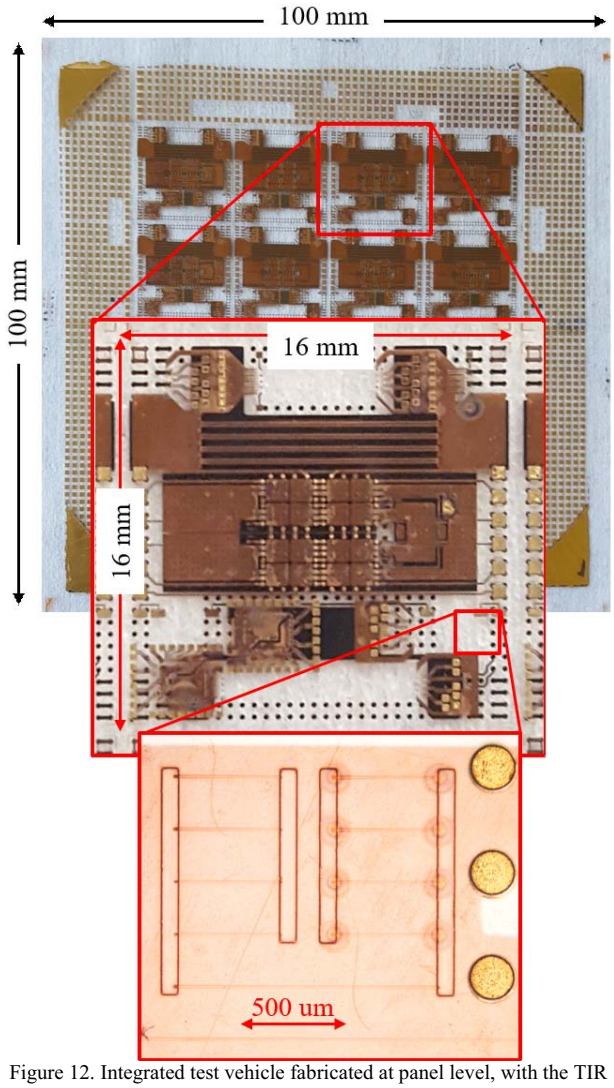

Figure 12. Integrated test vehicle fabricated at panel level, with the TIR turning mirror design implemented at 250 um pitch.

Acknowledgment

The authors would like to thank Professor Gee-Kung Chang, Dr. Daniel Guodotti, Rui Zhang, Chris White, Jialing Tong, Chandra Nair, Zihan Wu, and Jason Bishop from Georgia Tech for technical discussions and equipment support. The authors would like to acknowledge Michael Gallagher and Jeff Calvert from Dow Chemical for providing the CYCLOTENE™ materials and processing guidance. The authors would also like to acknowledge Aurelie Mayeux from MicroChem Corporation for providing the EPR-129 glass-glass bonding material. The authors would like to thank Frank Wei and Randall Clark from DISCO Corp. for their help in glass dicing. Last but not least, the authors would like to thank Michael Frankel and Jack Mateosky from Ciena Corporation, Jibin Sun and Terry Bowen from TE Connectivity, for helpful discussions on single-mode photonic interposer requirements.

REFERENCES

[1] M.A. Taubenblatt, "Optical Interconnects for High-Performance Computing," in *J. Lightw. Technol.*, vol.30, no.4, pp.448-457, Feb. 2012.

[2] Soref, R., "The Past, Present, and Future of Silicon Photonics," in *IEEE J. Select. Topics Quantum Electron.*, vol.12, no.6, pp.1678-1687, Nov.-dec. 2006.

[3] Ibrahim Murat Soganci, Antonio La Porta, and Bert Jan Offrein, "Flip-chip optical couplers with scalable I/O count for silicon photonics," *Opt. Express*, vol. 21, 16075-16085, 2013.

[4] W. S. Zaoui et al., "Cost-effective CMOS-compatible grating couplers with backside metal mirror and 69& coupling efficiency," *Opt. Express,* vol. 20, p. 6, Nov. 2012.

[5] B. Snyder, P. O'Brien, "Packaging Process for Grating-Coupled Silicon Photonic Waveguides Using Angle-Polished Fibers," in *IEEE Trans. Comp., Packag., Manufact. Technol.*, vol. 3, no. 6, pp. 954-959, June 2013

[6] M.S. Cohen et al., "Passive laser-fiber alignment by index method," in *Photonic Technology Letters*, vol. 3, pp. 985 – 987, 1991.

[7] L. Brusberg et al., "Thin Glass Based Electro-optical Circuit Board (EOCB) with Through Glass Vias, Gradient-index Multimode Optical Waveguides and Collimated Beam Mid-board Coupling Interfaces," in *IEEE 65th Electronic Components and Technology Conference (ECTC)*, San Diego, Ca, 2015, pp. 789-798.

[8] X. Dou et al., "Polymeric waveguides with embedded micromirrors formed by Metallic Hard Mold," in *Opt. Express*, vol. 18, p. 8, 2009.

[9] F. Doany *et al*., "Terabit/sec-class board-level optical interconnects through polymer waveguides using 24-channel bidirectional transceiver modules," in *IEEE 61st Electronic Components and Technology Conference (ECTC)*, Orlando, Fl, 2011, pp. 790–797.

[10] B. Chou et al., "Modeling, Design, and Demonstration of Ultra-miniaturized and High Efficiency 3D Glass Photonic Modules," in *IEEE 64th Electronic Components and Technology Conference (ECTC)*, Orlando, Fl, 2014.

[11] B. Chou et al., "Modeling, Design, Fabrication, and Characterization of Ultra-high Bandwidth 3D Glass Photonic Substrates," in *48th International Symposium on Microelectronics (IMAPS)*, Orlando, Fl, 2015.

[12] Y. Hirai et al., "Moving mask UV lithography for three-dimensional structuring," in *J. Micromech. Microeng.*, vol. 17, pp. 199-206, 2007.

[13] J. Calvert. "Enabling Materials Technology for Multi-Die Integration," presented at the *Microelectronics Packaging & Test Engineering Council (MEPTEC) Symposium*, San Jose, Ca, 2014.

[14] B. Sawyer *et al,* "Modeling, Design, and Demonstration of 2.5D Glass Interposers with 16x28 Gbps Signaling," in *IEEE 65th Electronic Components and Technology Conference (ECTC)*, San Diego, Ca, 2015.